Asian Journal of Chemistry; Vol. 26, No. 12 (2014), 3499-3503

ASIAN JOURNAL OF CHEMISTRY

http://dx.doi.org/10.14233/ajchem.2014.16102

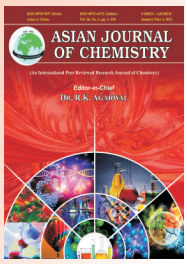

Novel MCR Synthesis of Post Transition Metal Complexes with Substituted Hydroxy Quinolines as Potent Antimicrobial Agent

ANSAR PERVAIZ[1], MUHAMMAD MAKSHOOF ATHAR[1], MISBAHUL AIN KHAN[1,2], ASHHAR UZ ZAMAN[1,*] and MUHAMMAD PERVAIZ[3]

[1]Institute of Chemistry, University of the Punjab, Lahore, Pakistan
[2]Department of Chemistry, University of Bahawalpur, Pakistan
[3]Department of Chemistry, Government College University, Faisalabad, Pakistan

*Corresponding author: Tel/Fax: +92 42 37164058 E-mail: ashhar47@hotmail.com

Received: 25 July 2013; *Accepted*: 11 September 2013; *Published online*: 5 June 2014; AJC-15281

A series of Ni(II), Cu(II) and Zn(II) complexes have been synthesized by condensation and cyclization methodology. The ligand was synthesized by MCR (multi component reaction) of *ortho* toluidine, ethyl acetoacetate and triethyl ortho-formate and the condensed product was further cyclized in dowtherm A. The synthesized ligand was reacted with $M(CH_3COO)_2$ (M = Ni, Cu or Zn), to get complexes. The synthesized metal complexes and ligand were characterized by FT-IR, Mass, X-ray crystallography and atomic absorption. The ligand as well as metal complexes were also screened for antimicrobial activities. The data showed that complexes exhibited more biological activities than ligand.

Keywords: Multi component reaction, Substituted quinolines, Metal complexes, *o*-Toluidine, 3-Acetyl-4-hydroxy-8-methylquinoline.

INTRODUCTION

Metal complexes with substituted quinolines especially copper, zinc and nickel complexes significantly reduce the decay of wood, cellulose and hemi cellulose, caused by fungi and used for wood preservative[1]. A process for treating such materials with these copper-containing antifungal agents is also disclosed. Copper(II) - complexes have octahedral, square pyramid and square planar geometries. They also reflect the strong coordinating ability for NO_3^-, Cl^-, Br^-, AcO^- and SO_4^{2-}, depending on the type of the anions. The zinc complexes of selected amino acids like proline, lysine, histidine, glycine and arginine can be used for inhibition of growth for the malarial parasite *i.e.*, *Plasmodium falciparum.* Zinc(II) complex has been shown to exhibit antimicrobial activity and ameliorate hyper insulinemia and massive hereditary obesity in mice. In addition to structural activity relationships of zinc complexes improved hyperglycemia and insulin resistance in diabetic mice. Zinc(II) complex actually triggered the development of new zinc complexes with anti-metabolic syndrome activity. Nickel occurs in various oxidation states and find wide applications in number of synthetic and biological mechanisms. A series of nickel complexes have been synthesized and employed for biological and fungal activities against different bacterial and fungal species[2-6]. The chelating power of nickel has been enhanced by treating it with several ligands[7]. Different studies revealed that nickel in +3 oxidation state can easily coordinate the quinoline derivative of ligands and showed remarkable antifungal and ant biological activities[2].

The post transition metals on complexing with certain ligands showed sufficient antimicrobial activities. The growth of different bacterial and fungal species has been restricted by transition metal complexes and data showed that ligands exhibited less biological and fungal activities than metal complexes[8]. The synthesized ligands and metal complexes are usually analyzed by various spectroscopic techniques such as FT-IR, Mass, NMR and X-ray crystallography[9].

EXPERIMENTAL

Analytical reagent grade chemicals and solvents including *ortho* toluidine, ethyl acetoacetate, triethyl orthofromate, copper acetate, zinc acetate, nickel acetate, toluene, acetic acid, ethanol, methanol, ethyl acetate were purchased from Sigma-Aldrich.

Characterization of synthesized ligands and metal complexes was done by using different spectroscopic tools. The ligands were analyzed by FT-IR, Mass, NMR and elemental analysis. The complexes were characterized on the single crystal X-ray diffraction, atomic absorption and FT-IR. The spectra for Fourier transform infrared (FT-IR) were recorded on Thermo FT-IR Nicolet IS 10 and Perkin Elmer FTIR. Electron ionization technique was used on Perkin Elmer Clarus 680

GC-MS instrument at 70ev for the mass spectra of ligands. JNM-ECX400 FT NMR 400 MHz System was engaged for ^{13}C NMR and $^{1}HNMR$ spectra of ligands.

Preparation of ligands: Equimolar quantities of ethylacetoacetate and triethylorthoformate were mixed in 250 mL flask and heated for 0.5 h at 120 °C. To this *ortho* toluidine was added and the mixtures were refluxed for 2 h at 80 °C and allowed to stay overnight for crystallization. The synthesized and crystallized product was washed with ethanol, filtered, dried and product was cyclized in Dowtherm A at 250 °C and diluted with *n*-hexane after cooling. The product was purified by washing with *n*-hexane and dried after filtration. Material was poured in 10 % 50 mL solution of KOH, stirred for 0.5 h and solution was filtered. Precipitation of the product was done by acidification with acetic acid and washed with water, dried to get desired ligand *i.e.*, 3-acetyl-4-hydroxy-8-methylquinoline (L). The yield of pure product was calculated 71 %.

Preparation of metal complexes: Stoichiometric quantities of post transition metals (cupric acetate, zinc acetate and nickel acetate) and ligand (L) were reacted separately in 1:2 molar ratio. The mixtures were refluxed in presence of methanol for 12 h, then were allowed to cool, filtered and dried (Fig. 1). The products were washed with methanol, re-crystallized and subjected for analysis.

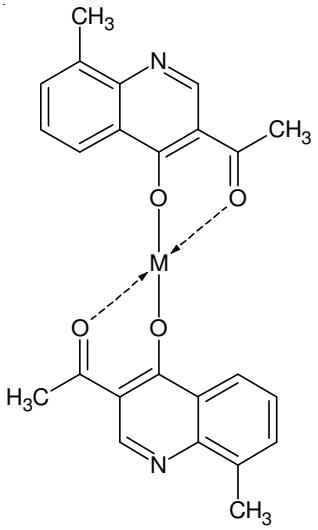

(M= Cu, Zn, Ni)

Fig. 1. structure of complex

Antibacterial activity: Different bacterial strains were used to check the antibacterial activity of ligands and metal complexes. The selected strains were *E. coli*, *B. subbtilis* and *S. aureus*. The most efficient method for antibacterial activity is disc diffusion method. In this method, water containing nutrient agar is homogenously dispersed and sterilized for 20 min at 121 °C in autoclave. Whole material is then transferred to Petri dish after reacting it with inoculums. Incubation of Petri plates was done at 37 °C for 24 h for bacterial growth on the discs of filter paper. These discs of filter papers were positioned parallel on growth medium and contain about 10 % (100 µL) of titled complexes and ligands. The metal complexes and ligands full of antibacterial activity inhibited the growth of bacteria and formed clear zones. Zone reader was used to determine the inhibition zones in millimeters[12]. Rifampicin was used as standard drug.

Antifungal activity: *A. flavus*, *A. alternate* and *A. niger* were the strains used to check the antifungal activities of ligands and metal complexes. The growth medium was synthesized, sterilized and then transferred to the Petri plates which were incubated for 48 h at 28 °C for fungus growth. Incubation started when each disc of filter paper contains 100 µL of each ligands and metal complexes. The metal complexes and ligands showed antifungal activities inhibited the growth of fungus and clear zones were produced[7]. The standard drug used was fluconazol[10].

RESULTS AND DISCUSSION

In IR spectra of the ligand, bending vibrations for C=O of acetyl group was observed at 1671.5 cm^{-1}. Ligand showed stretching and bending vibrations for aryl OH group at 3198.5 and 1342.4 and 1190.5, respectively. IR vibrations are given in Table-1.

^{1}H NMR: In spectra of ligand (L), peak at 2.709 ppm as singlet confirms three protons of methyl group at 8 position and peak at 2.504 ppm is due to three protons of acetyl group as singlet at 3 position in the molecule. Hydroxyl proton at 4 position showed peaks at 14.324 ppm. This high value is due to the strong electronegitivity of the oxygen atom attached thus desheilding the protons by attracting the electron density towards itself. Rest of the quinoline molecule contains four protons bonded to ring carbons and all these four protons have different environments and their peak values are given in the Table-2.

^{13}C NMR: In the ^{13}C NMR spectrum of the ligand (L) sp^3 hybridized carbon of methyl group at 8 position gave peak at 16.9 ppm and peak at 29.3 ppm is due to the sp^3 hybridized methyl carbon of acetyl group at 3 position of the molecule. Rest of the carbons of the molecule is sp^2 hybridized and absorbed in de-shielded region above 110 ppm. The carbon attached to oxygen through double bond in acetyl group is also sp^2 hybridized and due to the highly electronegative oxygen atom it absorbed in high de-shielded region and gave peak at 199.8 ppm. Spectral data is summarized in Table-3.

Mass spectrometry analysis: On the basis of earlier reported work ligand was characterized on mass spectrometry[11]. Molecular ion peak of ligand (L) was observed at 201 *m/z* with isotopic peak (almost 13 %) at 202 *m/z*. Base peak was

TABLE-1
CHARACTERISTIC IR FREQUENCIES OF LIGAND (L) AND METAL COMPLEXES OF (L)

		Absorption frequencies (cm^{-1})			
Functional group	Range (cm^{-1})	L	Cu- L	Zn-L	Ni-L
OH- str H-bonded	3200-3600	3198.5	–	–	–
C=O str	1650-1820	1671.5	1646.8	1668.2	1662.4
cis-Disubstituted alkenes	660-700	667.8 sharp	668.8 broad	664.5 broad	665.2 broad

TABLE-2
PROTON NMR OF LIGAND

No	Functional group/position of proton	Pattern	Value in ppm L
01	Acetyl protons at 3 position	singlet	2.504
02	Methyl protons at 8 position	singlet	2.709
03	Methoxy protons at 8 position	singlet	Not present
04	Proton at 2 position	singlet	9.250
05	Proton at 5 position	doublet	8.274
06	Proton at 6 position	triplet	7.795
07	Proton at 7 position	doublet	7.973
08	Proton at 8 position	singlet	Not present
09	Hydroxyl proton at 4 position	singlet	14.324

TABLE-3
^{13}C NMR OF LIGANDS

No	Functional group/position of Carbon	Peak area	Value in ppm L
01	Methyl carbon of acetyl group at 3 position	Single	29.3
02	Ketone carbon of acetyl group at 3 position	Single	199.8
03	Methyl carbon at 8 position of the molecule	Single	16.9
04	Carbon at 2 position of the molecule	Single	145.1
05	Carbon at 3 position of the molecule	Single	111.2
06	Carbon at 4 position of the molecule	Single	161.4
07	Carbon at 5 position of the molecule	Single	121.3
08	Carbon at 6 position of the molecule	Single	127.3
09	Carbon at 7 position of the molecule	Single	132.7
10	Carbon at 8 position of the molecule	Single	136.3
11	Carbon at 9 position of the molecule	Single	154.5
12	Carbon at 10 position of the molecule	Single	119.4
13	Methoxy carbon at 8 position of the molecule	Single	Not present

TABLE-4
CRYSTAL DATA FOR METAL COMPLEXES

Formula	$C_{24}H_{20}N_2Cu$	$C_{24}H_{20}N_2O_4Zn$	$C_{24}H_{20}N_2O_4Ni$
F. Wt.	463.987	465.850	459.134
Crystal Class	Monoclinic	Monoclinic	Monoclinic
Space Group C	2/c	2/c	2/c
a	26.632(5)	26.134(5)	25.968(5)
b	6.975(10)	6.845(10)	6.804(10)
c	14.708(2)	14.433(2)	14.341(2)
β	97.271(5)	97.271(5)	97.271(5)
Colour Formula	Light blue	White	Light green
Shape	Needle	Cubic	Needle
Volume	2759.0(7)	2698.0(7)	2733.0(7)
Z	4	4	4
Radiation type	Mo K_α	Mo K_α	Mo K_α
θ_{max}	28.92	28.92	28.92
H_{min}, H_{max}	-35 35	-35 35	-35 35
K_{min}, K_{max}	-8 8	-8 8	-8 8
L_{min}, L_{max}	-19 19	-19 19	-19 19
R-factor	0.05	0.05	0.05
Max shift/su	0.0003	0.0003	0.0003
Weighted R-factor	0.08	0.08	0.08
$\Delta\rho_{min}$	-1.69	-1.69	-1.69
$\Delta\rho_{max}$	2.92	2.92	2.92
Reflections used	3298	3284	3288
σ (I) limit	-10.00	-10.00	-10.00
Number of parameters	191	191	191
Goodness of fit	1.077	1.077	1.077

observed at 186 *m/z* with the cleavage of CH_3 group from molecular ion. This molecular ion fragment was further disintegrated by the cleavage of C=O group resulting in the fragment peak at 158 *m/z*. The fragment pattern of the molecule observed also by the further cleavage of methyl group at 8 position resulting peak at 143 *m/z* and followed by ring cleavage.

Infrared spectroscopy analysis: The functional groups of the complexes were confirmed by FTIR. On the basis of earlier reported work[12], IR absorption value for carbonyl group

was changed to the coordinate covalent bond of carbonyl oxygen with metal atom. Further the hydroxyl group showed a change in absorption frequencies due to oxygen and metal covalent bond. Also the ligands and complexes showed absorption arround 660 cm^{-1} (sharp) to 670 cm^{-1} (broad) respectively (Table-1).

XRD analysis of complexes: The structures of the complexes $[M(C_{12}H_{10}O_2N)_2]$ {where, M=Cu, Zn and Ni} were confirmed by X-ray crystallography. The crystallographic data and atom numbering scheme of the structures are shown in Tables 4-7.

XRD analysis of Cu-L complex: The molecular structure, selected bond lengths and bond angles are shown in Fig. 2 and Table-5. The crystal structure justify that titled complex is containing one metal atom. The metal atom is bonded to two oxygen atoms of hydroxyl group by covalent and two oxygen atoms of the acetyl group by coordinate covalent bonds to form distorted square planner geometry. The bond distances of Cu(31)-O(11) and Cu(31)-O(26) are 1.9069(1) nm and 1.92291(1) nm respectively. The bond length of Cu(31)-O(13) and Cu(31)-O(28) are longer with values 2.9934(1) and 2.9978(1), respectively which indicate that Cu(31)-O(13) and Cu(31)-O(28) are coordinate covalent bonds. The bond angles involving metal center for O(11)-Cu(31)-O(13), O(11)-Cu(31)-O(26), O(11)-Cu(31)-O(28), O(13)-Cu(31)-O(28), O(26)-Cu(31)-O(28) and O(26)-Cu(31)-O(13) are 50.32(3)°, 179.77(3)°, 130.01(3)°, 179.67(3)°, 50.22(3)°. and 129.45(3)°, respectively.

TABLE-5
SELECTED BOND LENGTHS (nm) AND ANGLES (°) FOR 2

Cu(1)-O(12)	Cu(1)-O(27)
1.7948(1)	1.8909(1)
Cu(1)-O(29)	Cu(1)-O(14)
2.9832 (1)	2.9046(1)
Co(19)-O(30)	O(12)-Cu(1)-O(27)
2.8332(7)	179.25(3)°
O(12)-Cu(1)-O(29)	O(12)-Cu(1)-O(14)
128.70(3)°	50.56(3)°
O(27)-Cu(1)-O(29)	O(29)-Cu(1)-O(14)
128.27(3)°	178.83(3)°

XRD analysis of Zn-L complex: The molecular structure, selected bond lengths and bond angles are shown in Fig. 3 and Table-6. The crystal structure justify that titled complex is containing one metal atom. The metal atom is bonded to two oxygen atoms of hydroxyl group by covalent and two oxygen atoms of the acetyl group by coordinate covalent bonds to form distorted square planner geometry. The bond distances of O(26)-Zn(31) and O(11)-Zn(31) are 1.9229(1) nm and 1.9069 (1) nm respectively. The bond length O(28)-Zn(31) and O(13)-Zn(31) are longer with values 2.9934(1) and 2.9978 (1), respectively which indicate that (28)-Zn(31) and O(13)-Zn(31) are coordinate covalent bonds. The bond angles involving metal center for O(26)-Zn(31)-O(11), O(26)-Zn(31)-O(28), O(26)-Zn(31)-O(13), O(11)-Zn(31)-O(28), O(11)-Zn(31)-O(13) and O(28)-Zn(31)-O(13) are 179.77(3)°, 50.22(3)°, 129.45(3)°, 130.01(3)°, 50.32(3)° and 179.67(3)°, respectively.

XRD analysis of Ni-L complex: The molecular structure, selected bond lengths and bond angles are shown in Fig 4 and

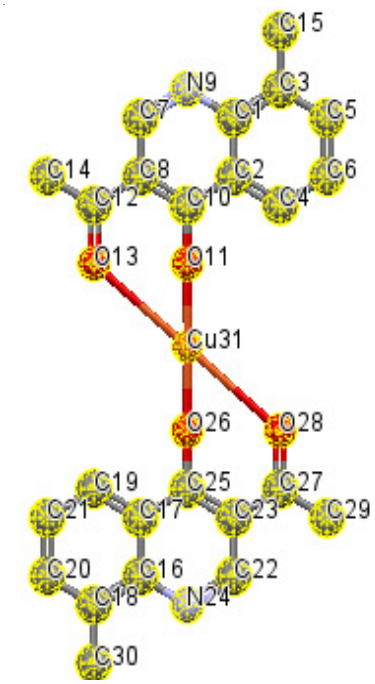

Fig. 2. A view of atomic numbering scheme of Cu metal complex at 50 % probability level of ellipsoid displacement

TABLE-6
SELECTED BOND LENGTHS (NM) AND ANGLES (°) FOR 3

O(26)-Ni(31)	O(11)-Ni(31)
1.9229(1)	1.9069(1)
O(28)-Ni(31)	O(13)-Ni(31)
2.9978(1)	2.9934(1)
O(26)-Ni(31)-O(11)	O(26)-Ni(31)-O(28)
179.77(3)°	50.22(3)°
O(26)-Ni(31)-O(13)	O(11)-Ni(31)-O(28)
129.45(3)°	130.01(3)°
O(11)-Ni(31)-O(13)	O(28)-Ni(31)-O(13)
50.32(3)°	179.67(3)°

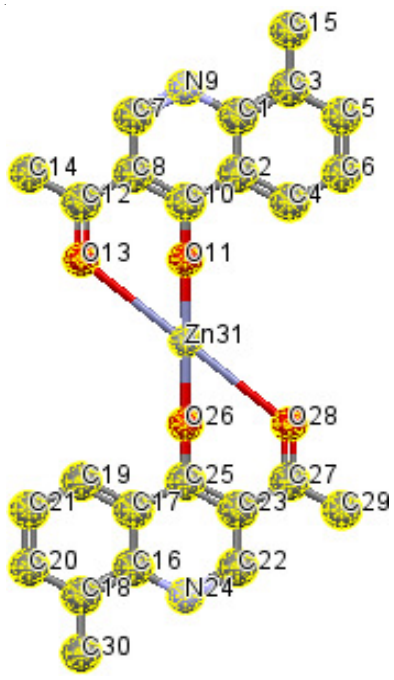

Fig. 3. A view of atomic numbering scheme of Zn metal structure at 50 % probability level of ellipsoid displacement

Table-7. The crystal structure justify that titled complex is containing one metal atom. The metal atom is bonded to two oxygen atoms of hydroxyl group by covalent and two oxygen atoms of the acetyl group by coordinate covalent bonds to form distorted square planner geometry. The bond distances of O(26)-Ni(31) and O(11)-Ni(31) are 1.9229 (1) nm and 1.9069 (1) nm respectively. The bond length O(28)-Ni(31) and O(13)-Ni(31) are longer with values 22.9978(1) and 2.9934(1), respectively which indicate that O(28)-Ni(31) and O(13)-Ni(31) are coordinate covalent bonds. The bond angles involving metal center for O(26)-Ni(31)-O(11), O(26)-Ni(31)-O(28), O(26)-Ni(31)-O(13), O(11)-Ni(31)-O(28), O(11)-Ni(31)-O(13) and O(28)-Ni(31)-O(13) are 179.77(3)° 50.22(3)° 130.01(3)°, 50.32(3)°, 50.22(3)°., 129.45(3)°, 130.01(3)°, 50.32(3)° and 179.67(3)°, respectively.

TABLE-7
SELECTED BOND LENGTHS (NM) AND ANGLES (°) FOR 4

O(26)-Zn(31) 1.9229(1)	O(11)-Zn(31) 1.9069 (1)
O(28)-Zn(31) 2.9978(1)	O(13)-Zn(31) 2.9934(1)
O(26)-Zn(31)-O(11) 179.77(3)°	O(26)-Zn(31)-O (28) 50.22(3)°
O(26)-Zn(31)-O(13) 129.45 (3)°	O(11)-Zn(31)-O(28) 130.01(3)°
O(11)-Zn(31)-O(13) 50.32(3)°	O(28)-Zn(31)-O(13) 179.67(3)°

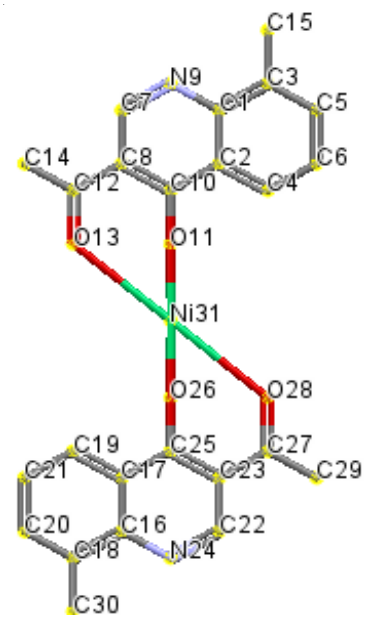

Fig. 4. A view of atomic numbering scheme of Ni metal structure at 50 % probability level of ellipsoid displacement

Antibacterial activity: The complex and ligand were tested for their antibacterial activity against different bacteria *via* disc diffusion method. The selected strains to test the antibacterial activities were *E. coli*, *S. aureus* and *Bacillus subtilis*. The ligand showed less activity as compared to metal complex. The highest activity was shown by ligand against *S. aureus* with zone 6 mm. The activity against *B. subtilis*, *E. coli* and were negligible with zone 4.25 mm and 4 mm, respectively. The maximum antibacterial activity was shown by complex against *E. coli* with zone 9 mm. The antibacterial activities of metal complex against *B. subtilis* and *S. aureus* were with zone 8 mm and 5.25 mm, respectively.

Antifungal activity: Different bacterial strains *i.e., A. flavis*, *A. alternate* and *A. niger* were engaged to check the antifungal activity of the metal complex and parental synthesized ligand by using disc method. The complex showed more significant activity than ligand. The maximum antifungal activity showed by ligand against *A. flavis* with zone 4.25 mm. The activity showed by *A. niger* was nil and *A. alternata* was 4 mm. The highest antifungal activity showed by metal complex against *A. alternata* with zone 12.25 mm and aginst *A. niger* and *A. flavis* were with zones 7.75 mm and 4 mm, respectively.

ACKNOWLEDGEMENTS

The authors thank Dr. Muhammad Wakeel Ahsan, Chief Executive of Bhatti Scientifics Lahore, Pakistan and Mr. Faisal Hameed from Biochemika International Lahore, Pakistan for support in research work.

REFERENCES

1. M.C. Burla, R. Caliandro, M. Camalli, B. Carrozzini, G.L. Cascarano, L. De Caro, C. Giacovazzo, G. Polidori and R. Spagna, *J. Appl. Cryst.*, **38**, 381 (2005).
2. N. Sultana, A. Naz, M.S. Arayne and M.A. Mesaik, *J. Mol. Struct.*, **969**, 17 (2010).
3. R.A. Chiarella, R.J. Davey and M.L. Peterson, *Cryst. Growth Des.*, **7**, 1223 (2007).
4. A.A.A. Abu-Hussen and W. Linert, *Synth. React. Inorg. Metal-Org. Nano-Metal Chem.*, **39**, 13 (2009).
5. R. Rajavel, M.S. Vadivu and C. Anitha, *E-J. Chem*, **5**, 620 (2008).
6. H.I. Ugras, I. Basaran, T. Kilic and U. Cakir, *J. Heterocycl. Chem.*, **43**, 1679 (2006).
7. M. Pervaiz, M. Yousaf, A. Jabbar, A.F. Zahoor, T.H. Bokhari, A. Anjum, M. Sagir, M.A. Khan, K.G. Ali, S. Ahmad, M. Zia-ur-Rehman, S. Ashraf and K.S. Qeureshi, *Asian J. Chem.*, **25**, 2161 (2013).
8. D. Singh, K. Kumar, S.S. Dhiman and J. Sharma, *J. Enzyme Inhib. Med. Chem.*, **25**, 21 (2010).
9. P.G. Cozzi, *Chem. Soc. Rev.*, **33**, 410 (2004).
10. M. Yousaf, M. Pervaiz, A.F. Zahoor, A.I. Hussain, M.K.K. Khosa, S. Ashraf, M. Sagir, Ashar-uz-Zaman and K. Shehzad, *Asian J. Chem.*, **25**, 521 (2013).
11. F. Dogan, M. Ulusoy, Ö. Öztürk, I. Kaya and B. Salih, *J. Therm. Anal. Calorim.*, **98**, 785 (2009).
12. M.F. Renehan, H.J. Schanz, E.M. McGarrigle, C.T. Dalton, A.M. Daly and D.G. Gilheany, *J. Mol. Catal. Chem.*, **231**, 205 (2005).